Asian Journal of Chemistry; Vol. 35, No. 2 (2023), 483-492

ASIAN JOURNAL OF CHEMISTRY

https://doi.org/10.14233/ajchem.2023.27002

Design, Synthesis and Anti-tubercular Evaluation of Some Novel Chroman-Hydrazone Derivatives

SAMAR MUJEEB[1], KULDEEP SINGH[2,*], BHUMIKA YOGI[1], PRAVEEN KUMAR[3] and PIYUSH KUMAR[4]

[1]Department of Pharmaceutical Chemistry, Hygia Institute of Pharmaceutical Education & Research, Lucknow-226020, India
[2]Department of Pharmaceutical Chemistry, Faculty of Pharmacy, Integral University, Lucknow-226021, India
[3]Faculty of Pharmacy, Uttar Pradesh University of Medical Sciences, Saifai-206130, Etawah, India
[4]Department of Chemistry, Indian Institute of Technology, Jammu, Jagti, NH-44, Nagrota, Jammu-181221, India

*Corresponding author: E-mail: kuldeep@iul.ac.in

Received: 5 December 2022; *Accepted*: 16 January 2023; *Published online*: 30 January 2023; AJC-21134

The molecular docking, synthesis, spectral characterization and anti-tubercular evaluation of 10 novel *N'*-substituted-6-hydroxy-2,5,7,8-tetramethylchroman-2-carbohydrazide derivatives (**SM1-SM10**) were reported. The structures of the synthesized derivatives were affirmed by spectroscopic studies such as FTIR, ^{1}H NMR, ^{13}C NMR and high resolution-mass spectrometry. Predicted ADME and toxicity investigations were accomplished to presume the pharmacokinetic parameters of the compounds. The synthesized compounds were evaluated for *in vitro* anti-tubercular activity against *Mycobacterium tuberculosis* H37Rv strain using Microplate Alamar Blue Assay (MABA) taking isoniazid, rifampicin, ethambutol, amikacin, streptomycin and levofloxacin as positive drug standards. Compound **SM8** has shown the significant anti-tubercular activity among all the titled compounds. The results indicated that chroman-hydrazone skeleton could serve as a lead for the development of novel anti-tubercular drugs.

Keywords: Anti-tubercular activity, Coumarin, hydrazone, Hybrid derivatives.

INTRODUCTION

Tuberculosis (TB) is an infectious disease which is caused by many species of *Mycobacterium*, collectively called tubercle bacilli or *Mycobacterium tuberculosis* complex. It is estimated that around 1.7 billion people are infected with *M. tuberculosis* around the world [1]. The rising drug resistance and severe adverse effects have created a thriving need to develop newer anti-tubercular drugs [2]. Multi-drug-resistant tuberculosis (MDR-TB) and extensively drug-resistant TB (XDR-TB) are challenging the current treatment of TB [3,4].

Coumarin is an intriguing class of oxygen heterocyclic compounds [5]. Chroman is a class of coumarin, which is endowed with the utmost medicinal value. Chroman ring is an integral part of many compounds reported of exhibiting remarkable anti-TB activity [6,7]. Pini *et al.* [8] synthesized chroman-based compounds as new potential inhibitors of *M. tuberculosis* and identified a novel lead compound. Many of the hydrazide-hydrazone derivatives have exhibited significant antibacterial-antifungal [9], anticonvulsant [10,11], anti-inflammatory [12] and antituberculosis activities [13,14]. Substituted carbohydrazone moiety is an active pharmacophore for many antituberculosis active molecules [15,16]. Motivated by these observations, we tried to gain a hybrid approach of combining chroman and hydrazide moiety to synthesize novel *N'*-substituted-6-hydroxy-2,5,7,8-tetramethylchroman-2-carbohydrazide scaffolds with substituted benzene groups. Trolox hydrazide was refluxed with different substituted aromatic aldehydes in the presence of ethanol and acetic acid for 8 h which underwent an addition-elimination reaction yielding 10 novel *N'*-substituted-6-hydroxy-2,5,7,8-tetramethylchroman-2-carbohydrazide derivatives. The hydrazone moiety was found to form many bonding interactions with the receptor protein of the mycobacterium.

A molecular docking study has been performed to get a fair idea about the preferred interaction, best conformation and binding modes made by our compounds with the target proteins and predict if the synthesized compound will be a good candidate as an anti-tubercular agent or not. Absorption, distribution, metabolism and elimination (ADME) and toxicity studies were also performed with the help of the SwissADME tool [17] to get an idea about the possible pharmacokinetic properties of

the synthesized compounds. Therefore, in present research, we report the docking studies, synthetic procedures and anti-tubercular activity of some novel chroman-hydrazones. These compounds were evaluated for their anti-tubercular potential on *M. tuberculosis, M. abscessus*, *M. fortuitum* and *M. chelonae.*

EXPERIMENTAL

All commercial chemicals were procured from Sigma-Aldrich and Spectrochem. Thin layer chromatography was conducted on E Merck silica gel GF-254 precoated plates and the identification was done under UV light. Melting points were determined in open glass capillaries and were reported uncorrected. NMR spectra were recorded on Bruker Avance 400/Av III HD-300 (FT NMR) in $CDCl_3$ at 300 MHz for ^1H NMR. The ^{13}C NMR was recorded in Bruker Av III HD-300 (FT NMR) in $CDCl_3$. The mass spectra were recorded with Waters Alliance e2695/HPLC-TQD Mass spectrometer using positive mode ESI and the *m/z* values are indicated in Dalton. The IR spectra (in KBr) were recorded on Perkin-Elmer Spectrum IR Version 10.7.2 spectrophotometer.

Synthesis of 6-hydroxy-2,5,7,8-tetramethyl-chroman-2-carboxylic acid methyl ester or Trolox ester (1): Methyl methacrylate (1.50 mol), paraformaldehyde (0.30 mol), dibutylamine (0.036 mol) and 4.5 mL of acetic acid were mixed in an round bottom flask. This mixture was stirred at room temperature and 0.30 mol of trimethyl hydroquinone was added later in this mixture. This reaction mixture was refluxed for 20 h with continuous stirring. At the end of reaction, this mixture was cooled down to 0-5 ºC and filtered. The dark brown colour product was obtained and washed with methanol several times to give light brown solid. This product was recrystallized from methanol to give light tan coloured solid.

Synthesis of 6-hydroxy-2,5,7,8-tetramethylchroman-2-carbohydrazide (2): Trolox ester (1 mmol) was refluxed along with 80% hydrazine hydrate (5 mmol) for 8-10 h taking ethanol as solvent. After the completion of reaction, the remaining solvent was evaporated in a water-bath and the resultant product was poured into cold water to obtain a white precipitate. The separated white solid was filtered, washed with distilled water and dried to obtain an off-white solid.

General procedure for the synthesis of chroman-hydrazones (3): A mixture of Trolox hydrazide **(2)** (1 mmol) and different aldehydes (1 mmol) with ethanol was taken in an round bottom flask and 3-4 drops of glacial acetic acid was added in the reaction mixture. The reaction was refluxed for 10-12 h. After completion of reaction, the reaction mixture was cooled at room temperature. The obtained resultant solid was then filtered, washed with cold ethanol and dried (**Scheme-I**). The compounds were further recrystallized by ethanol to obtain the final compounds **SM1-SM10**. The synthesized compounds were subjected to melting point analysis. The R_f value of all synthesized compounds was calculated in ethyl acetate and hexane (30:70) and ranges between 0.7-0.8.

***N′*-(2,6-Dichlorobenzylidene)-6-hydroxy-2,5,7,8-tetramethylchroman-2-carbohydrazide (SM1):** White needle like crystals. yield: 75%, m.p.: 175 ºC, R_f: 0.71, *m.f.*: $C_{21}H_{22}N_2O_3Cl_2$. IR (KBr, ν_{max}, cm^{-1}): 3345 (-OH), 1692 (>CO); ^1H NMR (300 MHz, $CDCl_3$, ppm): 9.188 (s, 1H, CH=N), 7.56 (s, 1H, -CONH-), 7.39-7.17 (m, 3H, Ar-H), 4.37 (s, 1H, -OH), 2.25 (s, 3H, $-CH_3$), 2.61-2.55 (m, 2H, $>CH_2$), 2.07 (s, 3H, $-CH_3$), 1.98 (s, 3H, $-CH_3$), 1.64 (m, 2H, $>CH_2$), 1.57 (s, 3H, $-CH_3$); ^{13}C NMR (300 MHz, $CDCl_3$): 170.2 (>CO), 152.1, 149.9, 144.2, 129.5, 121.9, 121.7, 119.3, 118.4, 111.8, 78.6, 77.6, 77.2, 76.8, 40.3, 29.8, 24.8, 20.6, 12.4, 12.3, 11.5; MS (*m/z*): 421.40 (M^+ for ^{35}Cl); 423.4 (M^+ for ^{37}Cl).

***N′*-(3-Methoxybenzylidene)-6-hydroxy-2,5,7,8-tetramethylchroman-2-carbohydrazide (SM2):** Brown crystals, yield: 80%, m.p.: 180 ºC, R_f: 0.80, *m.f.*: $C_{22}H_{26}N_2O_4$. IR (KBr, ν_{max}, cm^{-1}): 3367 (-OH), 1678 (>CO); ^1H NMR (300 MHz, $CDCl_3$, ppm): 9.34 (s, 1 H, CH=N), 8.01 (s, 1H, -CONH-), 7.34-7.33 (m, 1H, Ar-H), 7.27- 7.24 (t, *J* = 7.8 Hz, 1H, Ar-H), 7.21-7.18 (m, 1H, Ar-H), 6.96-6.92 (m, 1H, Ar-H), 4.40 (s, 1H, -OH), 3.82 (s, 3H, $-OCH_3$), 2.68-2.68 (m, 2H, $>CH_2$), 2.51-2.42 (m, 2H, $>CH_2$), 2.25 (s, 3H, $-CH_3$), 2.25 (s, 3H, $-CH_3$), 2.09 (s, 3H, $-CH_3$), 1.62 (s, 3H, $-CH_3$); ^{13}C NMR (300 MHz, $CDCl_3$): 170.9 (>C=O), 160.1, 149.3, 146.1, 134.9, 129.8, 122.0, 121.4, 119.3, 118.3, 117.9, 111.2, 78.7, 77.6, 77.2, 76.8, 55.6, 29.8, 24.8, 20.6, 12.4, 12.3, 11.5; MS (*m/z*): 383.50.

***N′*-(3-Nitrobenzylidene)-6-hydroxy-2,5,7,8-tetramethylchroman-2-carbohydrazide (SM3):** White shiny crystals, yield: 79%, m.p.: 185 ºC, R_f: 0.72, *m.f.*: $C_{21}H_{23}N_3O_5$. IR (KBr, ν_{max}, cm^{-1}): 3338 (-OH), 1684 (>CO); ^1H NMR (300 MHz, $CDCl_3$, ppm): 9.51 (s, 1 H, CH=N), 8.47- 8.46 (*J* = 3.6 Hz, t, 1H, Ar-H), 8.25-8.20 (*J* = 3 Hz, d, 1H, Ar-H), 8.13-8.10 (*J* = 7.8, d, 1H, Ar-H), 7.59-7.54 (*J* = 15.9, t, 1H, Ar-H), 7.26 (s, 1H, -CONH-), 4.44 (s, 1H, -OH), 2.69-2.63 (m, 2H, $>CH_2$), 2.51-2.42 (m, 2H, $>CH_2$), 2.26 (s, 3H, $-CH_3$), 2.20 (s, 3H, $-CH_3$), 2.09 (s, 3H, $-CH_3$), 1.63 (s, 3H, $-CH_3$); ^{13}C NMR (300 MHz, $CDCl_3$): 171.3 (>C=O), 148.8, 146.6, 146.2, 144.0, 135.7, 132.9, 129.9, 125.0, 122.7, 122.0, 121.8, 119.4, 118.2, 78.7, 77.6, 77.2, 76.8, 29.8, 24.7, 20.5, 12.4, 12.3, 11.5; MS (*m/z*): 398.50.

***N′*-(4-Nitrobenzylidene)-6-hydroxy-2,5,7,8-tetramethylchroman-2-carbohydrazide (SM4):** Yellow shiny crystals, yield: 77%, m.p.: 170 ºC, R_f: 0.70, *m.f.*: $C_{21}H_{23}N_3O_5$. IR (KBr, ν_{max}, cm^{-1}): 3367 (-OH), 1685 (>CO); ^1H NMR (300 MHz, $CDCl_3$, ppm): 9.54 (s, 1 H, CH=N), 8.26 (s, 1H, -CONH-), 8.23-8.21 (*J* = 6.3, d, 2H, Ar -H), 7.88-7.85 (*J* = 6.3, d, 2H, Ar-H), 4.46 (s, 1H, -OH), 2.72-2.63 (m, 2H, $>CH_2$), 2.50-2.41 (m, 2H, $>CH_2$), 2.25 (s, 3H, $-CH_3$), 2.20 (s, 3H, $-CH_3$), 2.209 (s, 3H, $-CH_3$), 1.62 (s, 3H, $-CH_3$); ^{13}C NMR (300 MHz, $CDCl_3$): 171.4 (>C=O), 148.9, 146.4, 146.3, 144.0, 139.8, 128.4, 124.1, 122.0, 121.9, 119.4, 118.1, 78.7, 77.6, 77.2, 76.8, 29.2, 24.7, 20.5, 12.4, 12.3, 11.5; MS (*m/z*): 398.50.

***N′*-(2-Bromobenzylidene)-6-hydroxy-2,5,7,8-tetramethylchroman-2-carbohydrazide (SM5):** Dark yellow crystals, yield: 85%, m.p.: 145 ºC, R_f: 0.76, *m.f.*: $C_{21}H_{23}N_2O_3Br$. IR (KBr, ν_{max}, cm^{-1}): 3377 (-OH), 1683 (>CO); ^1H NMR (300 MHz, $CDCl_3$, ppm): 9.95 (s, 1 H, CH=N), 8.45 (s, 1H, -CONH-), 4.37 (s, 1H, -OH), 8.12-8.09 (*J* = 9.3, dd, 1H, Ar-H), 7.55-7.52 (*J* = 9, dd, 1H, Ar-H), 7.33-7.28 (*J* = 9.3, t, 1H, Ar-H), 7.22-7.19 (*J* = 9.3, t, 1H, Ar-H), 2.69-2.64 (m, 2H, $>CH_2$), 2.51-2.42 (m, 2H, $>CH_2$), 2.26 (s, 3H, $-CH_3$), 2.20 (s, 3H, $-CH_3$), 2.21 (s, 3H, $-CH_3$), 1.62 (s, 3H, $-CH_3$); ^{13}C NMR (300 MHz, $CDCl_3$):

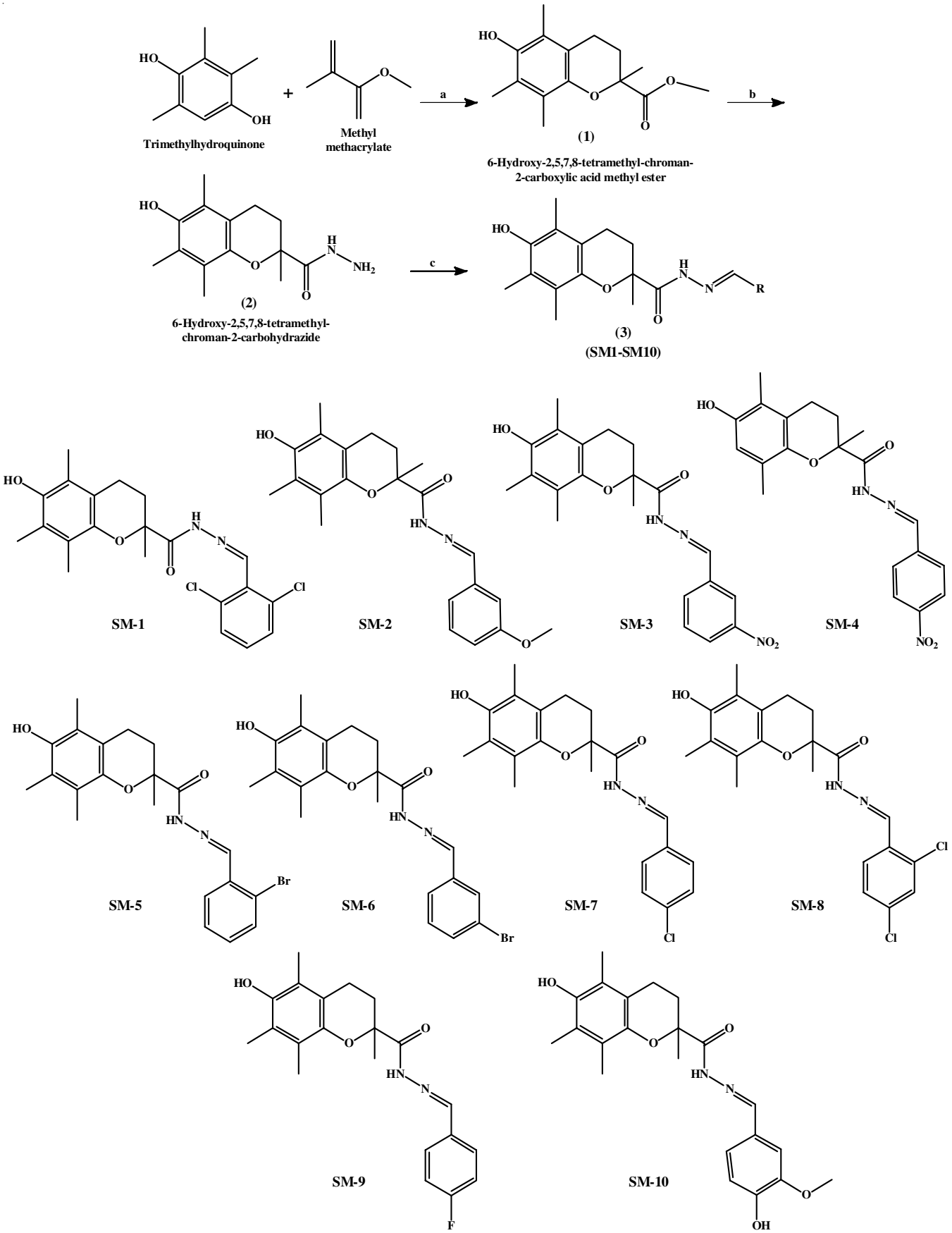

Scheme-I: Synthetic pathway for compounds **SM1-SM10**. (a) $(HCHO)_n$, $[CH_3(CH_2)_3]_2NH$, CH_3COOH, reflux, 20 h; (b) $NH_2NH_2{\cdot}H_2O$, EtOH, reflux, 10 h; (c) Substituted benzaldehyde, EtOH, CH_3COOH, reflux, 10-12 h

171.0 (>C=O), 147.8, 146.2, 144.1, 133.2, 132.5, 131.9, 128.6, 127.8, 124.5, 122.1, 121.8, 119.3, 118.3, 78.7, 77.6, 77.2, 76.8, 29.8, 24.7, 20.5, 12.4, 12.3, 11.52. MS (*m/z*): 433.40 (M^+ for ^{79}Br); 434.5 (M^+ for ^{81}Br).

***N'*-(3-Bromobenzylidene)-6-hydroxy-2,5,7,8-tetramethylchroman-2-carbohydrazide (SM6):** Off white crystals, yield: 70%, m.p.: 175 ºC, R_f: 0.86, *m.f.*: $C_{21}H_{23}N_2O_3Br$. IR (KBr, ν_{max}, cm^{-1}): 3342.31 (-OH), 1680 (>CO); ^1H NMR (300 MHz, $CDCl_3$, ppm): 9.39 (s, 1 H, CH=N), 8.00 (s, 1H, -CONH-), 7.91-7.90 (*J* = 3.3, t, 1H, Ar-H), 7.62-7.59 (*J* = 7.8, m, 1H, Ar-H), 7.52-7.48 (m, 1H, Ar-H), 4.41 (s, 1H, -OH), 2.72-2.63 (t, 2H, $>CH_2$), 2.51-2.42 (m, 2H, $>CH_2$), 2.25 (s, 3H, $-CH_3$) 2.20 (s, 3H, $-CH_3$), 2.209 (s, 3H, $-CH_3$), 1.62 (s, 3H, $-CH_3$). ^{13}C NMR (300 MHz, $CDCl_3$): 170.6 (>C=O), 161.3, 149.1, 146.11, 144.2, 129.6, 126.0, 122.0, 121.7, 119.3, 118.3, 114.8, 78.6, 77.6, 77.2, 76.8, 63.8, 29.8, 24.8, 20.6, 14.9, 12.4, 12.3, 11.5. MS (*m/z*): 435.59.

***N'*-(4-Chlorobenzylidene)-6-hydroxy-2,5,7,8-tetramethylchroman-2-carbohydrazide (SM7):** Off white crystals, yield: 70%, m.p.: 177 ºC, R_f: 0.77, *m.f.*: $C_{21}H_{23}N_2O_3Cl$. IR (KBr, ν_{max}, cm^{-1}): 3339 (-OH), 1685 (>CO); ^1H NMR (300 MHz, $CDCl_3$, ppm): 9.617 (s, 1 H, CH=N), 8.580 (s, 1H, -CONH-), 8.28-8.24 (dd, 1H, Ar-H), 8.05-8.02 (dd, 1H, Ar-H), 7.67-7.62 (m, 1H, Ar-H), 7.56-7.51 (m, 1H, Ar-H), 4.40 (s, 1H, -OH), 2.69-2.65 (t, 2H, $>CH_2$), 2.51-2.42 (m, 2H, $>CH_2$), 2.25 (s, 3H, $-CH_3$), 2.20 (s, 3H, $-CH_3$), 2.10 (s, 3H, $-CH_3$), 1.63 (s, 3H, $-CH_3$); ^{13}C NMR (300 MHz, $CDCl_3$): 171.0 (>C=O), 147.9, 129.2, 129.0, 118.3, 78.7, 77.6, 77.2, 76.8, 29.8, 24.8, 20.6, 12.4, 12.3, 11.5. MS (*m/z*): 387.54 (M^+ for ^{35}Cl); 389.5 (M^+ for ^{37}Cl).

***N'*-(2,4-Dichlorobenzylidene)-6-hydroxy-2,5,7,8-tetramethylchroman-2-carbohydrazide (SM8):** Off white crystals, yield: 78%, m.p.: 185 ºC, R_f: 0.80, *m.f.*: $C_{21}H_{22}N_2O_3Cl_2$. IR (KBr, ν_{max}, cm^{-1}): 3385 (-OH), 1681.67 (>CO); ^1H NMR (300 MHz, $CDCl_3$, ppm): 9.52 (s, 1 H, CH=N), 8.40 (s, 1H, -CONH-), 8.08-8.06 (d, *J* = 8.4, 1H, Ar-H), 7.378-7.371 (d, *J* = 2.1, 1H, Ar-H), 7.26-7.23 (d, *J* = 10.2, 2H, Ar-H), 4.44 (s, 1H, -OH), 2.68-2.63 (m, 2H, $-CH_2$), 2.50-2.42 (m, 2H, 3-CH_2), 2.25 (s, 3H, $-CH_3$) 2.20 (s, 3H, $-CH_3$), 2.09 (s, 3H, $-CH_3$), 1.62 (s, 3H, $-CH_3$); ^{13}C NMR (300 MHz, $CDCl_3$): 171.1 (>CO), 146.2, 144.3, 144.0, 137.0, 134.9, 129.8, 129.7, 128.9, 127.8, 122.0, 121.8, 119.3, 118.2, 78.7, 77.6, 77.2, 76.8, 29.8, 24.7, 20.5, 12.4, 12.3, 11.5. MS (*m/z*): 421.47 (M^+ for ^{35}Cl); 423.52 (M^+ for ^{37}Cl).

***N'*-(4-Fluorobenzylidene)-6-hydroxy-2,5,7,8-tetramethylchroman-2-carbohydrazide (SM9):** Buff-brown crystals, yield: 75%, m.p.: 180 ºC, R_f: 0.80, *m.f.*: $C_{21}H_{23}N_2O_3F$. IR (KBr, ν_{max}, cm^{-1}): 3340 (-OH), 1678 (>CO); ^1H NMR (300 MHz, $CDCl_3$, ppm): 9.33 (s, 1 H, CH=N), 8.02 (s, 1H, -CONH-), 7.73-7.69 (m, 2H, Ar-H), 7.09-7.03 (m, 2H, Ar-H), 4.40 (s, 1H, -OH), 2.68-2.63 (m, 2H, $>CH_2$), 2.50-2.42 (m, 2H, $>CH_2$), 2.30-2.17 (m, 6H, $-CH_3$), 2.09 (s, 3H, $-CH_3$), 1.62 (s, 3H, $-CH_3$); ^{13}C NMR (300 MHz, $CDCl_3$): 170.9 (>CO), 147.9, 146.1, 144.0, 129.9, 129.8, 121.9, 121.7, 119.3, 118.2, 116.2, 115.9, 78.6, 77.6, 77.4, 77.2, 76.8, 29.7, 24.7, 20.5, 12.4, 12.3, 1.5. MS (*m/z*): 371.56.

***N'*-(4-Hydroxy-3-methoxybenzylidene)-6-hydroxy-2,5,7,8-tetramethylchroman-2-carbohydrazide (SM10):** Off white crystals, yield: 80%, m.p.: 170 ºC, R_f: 0.60, *m.f.*: $C_{22}H_{26}N_2O_5$. IR (KBr, ν_{max}, cm^{-1}): 3341 (-OH), 1670 (>CO); ^1H NMR (300 MHz, $CDCl_3$, ppm): 9.25 (s, 1 H, CH=N), 7.93 (s, 1H, -CONH-), 7.65-7.62 (d, 2H, Ar-H), 6.88-6.85 (d, 2H, Ar-H), 3.66 (s, 1H, -OH), 2.67-2.62 (m, 2H, $>CH_2$), 2.50-2.42 (m, 2H, $>CH_2$), 2.25 (s,3H, $-CH_3$), 2.20 (s, 3H, $-CH_3$), 2.21 (s, 3H, $-CH_3$), 2.08 (s, 3H, $-CH_3$),), 2.09 (s, 3H, $-CH_3$), 2.01-1.94 (m, 2H, $-CH_2$), 1.61 (s, 3H, $-CH_3$), 1.43-1.38 (s, 3H, $-CH_3$); ^{13}C NMR (300 MHz, $CDCl_3$): 170.7 (>CO), 149.4, 148.6, 147.3, 146.1, 126.0, 124.0, 121.7, 119.3, 118.3, 114.2, 108.1, 78.6, 77.6, 77.4, 77.2, 76.8, 56.4, 29.8, 24.8, 20.6, 12.4, 12.3, 11.5. MS (*m/z*): 399.61.

Anti-tubercular evaluation: The synthesized compounds were tested against $MTBH_{37}Rv$ (ATCC-27294) strain in BACTEC 12 B medium, using the Microplate Alamar Blue Assay (MABA). The positive drug standard compounds taken were isoniazid, rifampicin, streptomycin, ethambutol, levofloxacin and amikacin at concentrations of 0.03, 0.06, 0.125, 0.25, 0.5, 1, 2, 4, 8, 16, 32 and 64 µg/mL. Before moving, the plates were kept aside to reach room temperature. Dried in a clean, laminar-flow cabinet. Each bacterial suspension (5 µL) from each strain was added to the surface of culture medium as an inoculum (usually 15-20 drops per plate). Until the drops were absorbed, plates were placed in a sterile laminar flow cabinet. The plates were then incubated at a 5% CO_2 incubator for 48 h at 36 ºC in a humid chamber. After incubation, each strain developed on the control plate without antibiotics. The pink colour on the plate confirmed the bacterial growth, whereas the blue colour indicated that no bacterial growth was present.

***In silico* molecular docking studies:** Docking studies were performed to determine the best conformation, preferred interactions and binding modes with the target protein of Mtb. The docking was performed by taking two target proteins (PDB ID: 3PTY) and (PDB ID: 4FDO). The crystal structures of proteins were collected from Protein Data Bank (reference from rcsb). The docking was performed with the help of AutoDock Vina [18,19] which is an open-source docking program for drug discovery, molecular docking and virtual screening and results were visualized by Discovery studio [20] and PyMol tool.

Collection and preparation of data: The 2D structures of the suggested analogues were designed by molecular graphics software ChemDraw and were later converted into the 3D format by Avogadro molecular editor. The designed analogues were converted into their PDB format with the help of the Open-Babel tool. AutoDock Vina was used to convert the PDB format of the designed molecules into their PDBQT format.

Target proteins: Crystal structure of *Mycobacterium tuberculosis* DprE1 in complex with CT319 (PDB ID: 4FDO) [21] and crystal structure of the C-terminal extracellular domain of *Mycobacterium tuberculosis* EmbC (PDB ID: 3PTY) [22] were both retrieved from the Protein Data Bank.

The protein structures were processed by removing all the water molecules (water without H-bonds), bound ligands, buffers, *etc*. The polar hydrogens were assigned to the protein and Kollman charges were added. Torsions were introduced using AutoDock after structural strain reduction and 3D structural correction were performed using the Merck method of force field (MMFF). AutoGrid was used for the generation of the grid map using a grid box. The grid spacing of 1 Å was chosen

and the grid centre was assigned at dimensions (x, y and z): 39.274, 9.529 and 8.675 for 4FDO protein and grid dimensions (x, y and z): 84.262. 5.096, 13.684 were designated for 3PTY protein. An exhaustiveness of 8 was chosen for each grid box.

Visualization of docking results: The optimized ligands were docked into target proteins considering both the protein and ligands as rigid. AutoDock Vina was run and the best energy favourable pose was saved. The pose with the lowest binding energy or binding affinity was selected and the interactions of the protein-ligand complex were visualized using the discovery Studio visualize tool and PyMOL tool.

RESULTS AND DISCUSSION

The synthesis of Trolox ester was done by reported methods [23]. The synthesis of 6-substituted-2,5,7,8-tetramethyl-3,4-dihydro-2*H*-chroman-2-carbohydrazide [24] was described in the experimental section. A mixture of Trolox hydrazide (**2**; 1 mmol) and different aldehydes (1 mmol) was taken in an round bottom flask with ethanol and 4-5 drops of glacial acetic acid was added to the reaction mass. The reaction was refluxed for 10-12 h. After the reaction came to end, the reaction mixture was cooled and ice-cold water was poured into it. The obtained white precipitate was then filtered, dried and recrystallized with ethanol.

Synthetic mechanism: A feasible mechanism explaining the reaction is depicted in **Scheme-II**. It may be speculated that step I of reaction involved the nucleophilic attack of hydrazine hydrate at the ester group of Trolox ester (**I**) leading to the formation of Trolox hydrazide (**III**). Large excess was taken to facilitate the removal of -OCH_3. The next step is the addition-elimination reaction where Trolox hydrazide is attacked by the carbonyl group of aldehyde and it undergoes an addition reaction by bond formation between the nitrogen of hydrazide and carbon of aldehydic carbonyl group forming an unstable intermediate (**V**). The intermediate (**V**) shows keto-enol tautomerism and interconvert itself into intermediate (**VI**), which again undergoes dehydration followed by subsequent deprotonation (**VII**) in the next step and leads to the formation of an imine (**VIII**) as the final product.

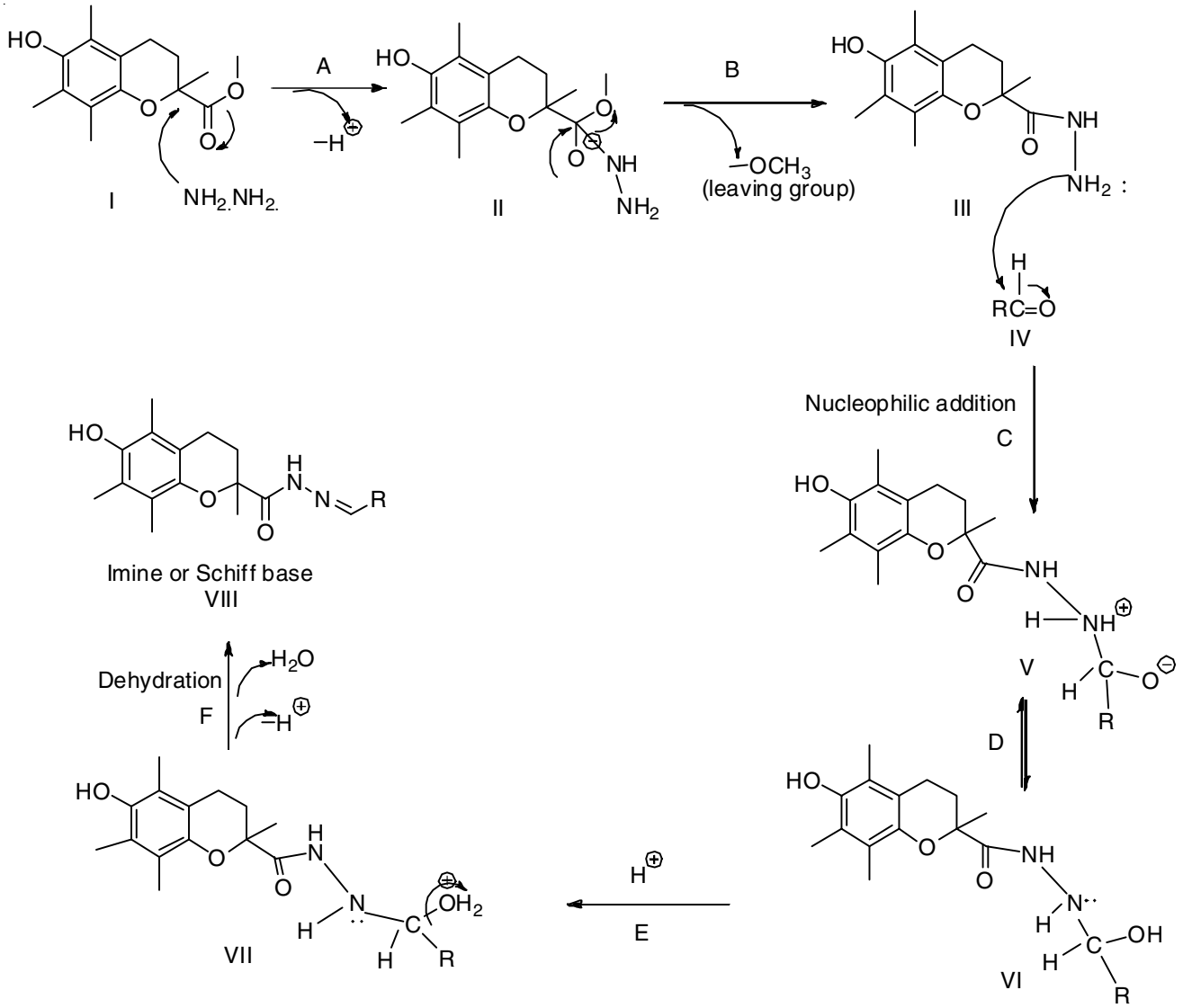

Scheme-II: Reaction mechanism of the synthetic scheme

All the synthesized compounds were characterized by IR, ^{1}H NMR, ^{13}C NMR and mass spectral analysis. The spectral data of newly synthesized compounds (**SM1-SM10**) were in good agreement with the proposed structures. The IR spectra of the compounds displayed a characteristic absorption band between 1695-1670 cm^{-1} (*str.*), which correlated to >C=O group of amide (–CONH-). All compounds displayed a broad absorption band at 3424-3330 cm^{-1} of the hydroxyl group (-OH, *str.*). In ^{1}H NMR, the most downfield signal at δ 9.18-9.95 ppm was observed corresponding to the proton of imine group (CH=N). The next most downfield singlet was observed at δ 7.5-8.5 ppm, which corresponded to the proton of amide (–CONH-) group. The broad small sharp singlet peak was observed in the rather upfield region of spectra at δ 3.66-4.46 ppm, which confirmed the hydroxyl group (-OH) in the compounds. All of the other aromatic and aliphatic protons were present at their marked position. The aromatic protons of the phenyl ring showed a resonance multiplet in the range of δ 8.4-7.4 ppm, which was de-shielded due to the presence of electronegative groups. Tall singlets were observed at the highly shielded region of the spectra between δ 2-3 ppm which corresponded with the methyl groups at the coumarin ring. Small multiplets of $–CH_2$ were seen between δ 2.68-2.2 ppm which were corresponding to the non-benzene coumarin ring protons. All the signals were found to correspond to their established structures. In ^{13}C NMR, the signal due to the carbonyl of the amide group (C=O) appeared at δ 169.7-172 ppm. The mass spectra of almost all compounds were found in agreement with the molecular weight of the compounds.

***In vitro* anti-tubercular evaluation:** The synthesized compounds were assessed *in vitro* for their potential to inhibit the growth of *M. tuberculosis* H37Rv by Microplate Alamar Blue Assay (MABA) [25]. Isoniazid, rifampicin, streptomycin, ethambutol, levofloxacin and amikacin were taken as standard drugs. The *in vitro* anti-mycobacterial screening results were enunciated as minimal inhibition concentration (MIC) in μg/mL and are compiled in Table-1. Amongst the series, compound **SM8** emerged as a highly propitious anti-tubercular agent by inhibiting the growth of *M. tuberculosis* at MIC = 16 μg/mL. Compounds **SM4** and **SM7** exhibited significantly fair anti-tubercular activity with MIC = 32 μg/mL. Compounds **SM1**, **SM5**, **SM6** and **SM9** were also found to be active anti-tubercular agents with MIC = 64 μg/mL. Compounds **SM5**, **SM6** and **SM9** were found broad-spectrum anti-tubercular agents as they were effective against *M. fortuitum* and *M. chelonae.* Most of the titled compounds have shown promising anti-tubercular activity and could be used as template in development of newer anti-tubercular agents.

Structure-activity relationship (SAR) analysis: The SAR study reveals that the introduction of the substituted phenyl ring with electron-withdrawing groups along with the chroman moiety lead to the enhanced anti-tubercular activity of the compounds. The electron-withdrawing groups particularly halogens (Br, Cl, F) and the nitro group contributed to the anti-tubercular activity of the synthesized derivatives. The disubstituted chlorine (2,4-dichloro) group in **SM8**, (2,6-dichloro) in **SM1** and mono-substituted chlorine (4-chloro) in **SM7** reinforced anti-tubercular activity in the molecules. However, dichloro substitution lead to better activity than the mono-chloro substitution and also slight change from 2,6 position to 2,4 position of two chlorine atoms leads to enhanced activity, which might have changed the binding orientation of the molecule at the receptor site. Bromo substitution in compounds **SM5** and **SM6** manifested fair anti-tubercular activity. Halogen increases the lipophilicity of the molecules, making them broad and more polarized. Due to which london dispersion forces get magnified and interactions among the lipophilic substance with other substituents get improved. Significant anti-tubercular activity of compound **SM4** may be attributed to the nitro group, which provides hydrogen-bonding atoms and imparts the lipophilicity to the molecule, resulting in the increased substrate-inhibitor interactions. Among the nitro-substituted derivatives (**SM3** and **SM4**), the *para* nitro-substituted derivative (**SM4**) was found to be more active as compared with the *ortho*-substituted one (**SM3**). The reason could be attributed to the overall stereochemistry and mode of binding at the target active site as predicted by docking. Compounds (**SM2** and **SM10**) substituted with the methoxy group ($-OCH_3$) have shown very weak anti-tubercular activity as compared to other compounds in the series. The possible reason behind this could be the very moderate effect of the methoxy group on the molecular hydrophobicity.

TABLE-1
ANTI-TUBERCULAR SCREENING RESULTS OF THE SYNTHESIZED COMPOUNDS (**SM1-SM10**)

Code	MIC (μg/mL)			
	M. tuberculosis H37Rv ATCC 27294	*M. abscessus* ATCC 19977	*M. fortuitum* ATCC 6841	*M. chelonae* ATCC 35752
SM1	64	>64	>64	>64
SM2	>64	>64	>64	>64
SM3	>64	>64	>64	>64
SM4	32	>64	>64	>64
SM5	64	>64	64	64
SM6	64	>64	64	64
SM7	32	>64	>64	>64
SM8	16	>64	64	>64
SM9	64	>64	>64	>64
SM10	>64	>64	>64	>64
Isoniazid	0.03	NT	NT	NT
Rifampicin	0.06	NT	NT	NT
Streptomycin	0.5	NT	NT	NT
Ethambutol	1	NT	NT	NT
Levofloxacin	0.25	2	0.06	0.12
Amikacin	0.12	8	1	2

Visualization of the docking results: Compound **SM8** has shown the best anti-tubercular activity among all the synthesized compounds and it has shown decent binding scores (-4.6 Kcal/mol) and (-9.7 Kcal/mol) with both the target proteins 3PTY and 4FDO, respectively. However, compound **SM9** has shown the highest binding score with the target protein (PDB ID:3PTY), whereas compound **SM4** has shown the best binding score with the target protein (PDB ID:4FDO). As depicted in Table-2, compound **SM9** with a binding affinity of -6.4 kcal/mol for (PDB ID:3PTY), has shown an even better binding score than isoniazid and ethambutol. All of the analogues gave

TABLE-2
DOCKING SCORE (KCAL/MOL) OF THE COMPOUNDS **SM1-SM10** WITH (PDB: 3PTY) AND (PDB: 4FDO)

Standard drugs and titled compounds	PDB: 3PTY	PDB: 4FDO
Ethambutol	-6.0	-6.9
Isoniazid	-6.0	-6.5
SM1	-5.8	-10.3
SM2	-4.3	-9.7
SM3	-3.7	-10.1
SM4	-4.1	-11.8
SM5	-5.7	-7.3
SM6	-4.0	-9.9
SM7	-5.5	-10.9
SM8	-4.6	-9.7
SM9	-6.4	-11.1
SM10	-4.3	-9.9

much better binding scores than the reference drugs isoniazid (-6.5 kcal/mol) and ethambutol (6.9 kcal/mol) for the target protein (PDB ID:4FDO). The analogue **SM4** (-11.8 kcal/mol), **SM7** (10.9 kcal/mol)) and **SM9** (-11.1 kcal/mol) has shown a very good binding score with the target protein (PDB ID: 4FDO) which is in correspondence with the anti-tubercular activities of the analogues.

Binding interaction of SM8 with target protein (PDB ID: 4FDO): Fig. 1 depicts the binding poses and interactions of compound **SM8** with the target protein (PDB ID: 4FDO), the compound **SM8** has made a hydrogen bond interaction with the amino acid residue GLY-117 with a bond length of 2.37 Å. The hydrogen bond was raised from the oxygen atom of the coumarin moiety. It has also made two pi-alkyl bonding interactions with LEU-363 and LYS-134 amino-acid residues with a bond distance of 3.24 and 4.60 Å, respectively. The interaction are raising from methyl groups of chroman moiety. Three alkyl pi-alkyl bonding interactions with the VAL-365 residue of the protein were observed raising from the two chlorine atoms present on the non-chroman benzene ring. Compound **SM8** has shown the best anti-tubercular activity and supposed to be due to its multiple bonding interactions with the target proteins.

Binding interaction of SM8 with target protein (PDB ID: 3PTY): As depicted in Fig. 2a-d, compound **SM8** forms multiple binding interactions with the target protein (PDB ID: 3PTY). It forms a hydrogen bond interaction with the TYR-841 residue of the protein. The hydrogen bond was raised from the nitrogen of the N-N=C bond with a bond distance of 2.38 Å. Pi-alkyl and carbon-hydrogen bonds interactions were observed

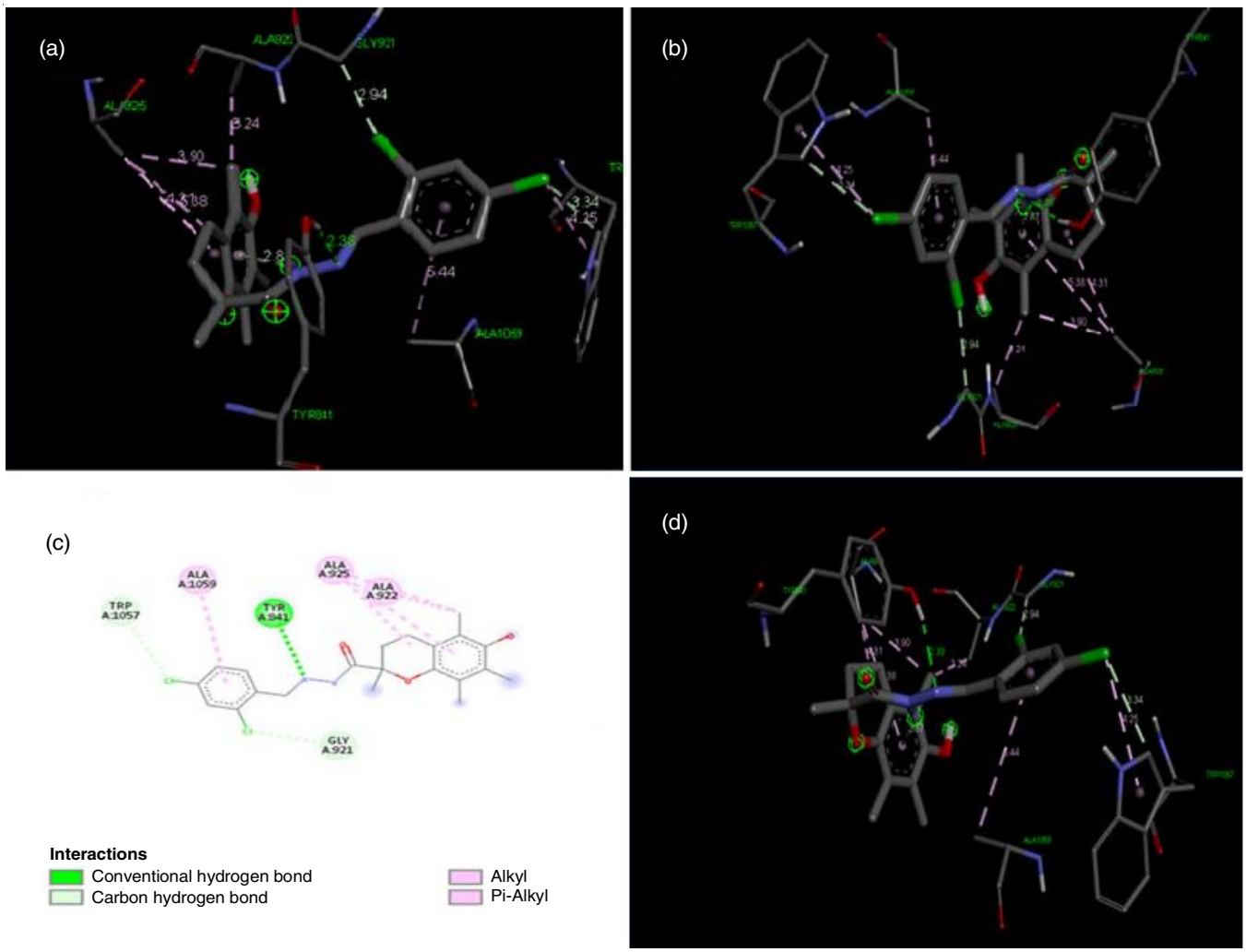

Fig. 1. Binding interactions of the docked ligand **SM8** with the target protein (PDB ID: 4FDO)

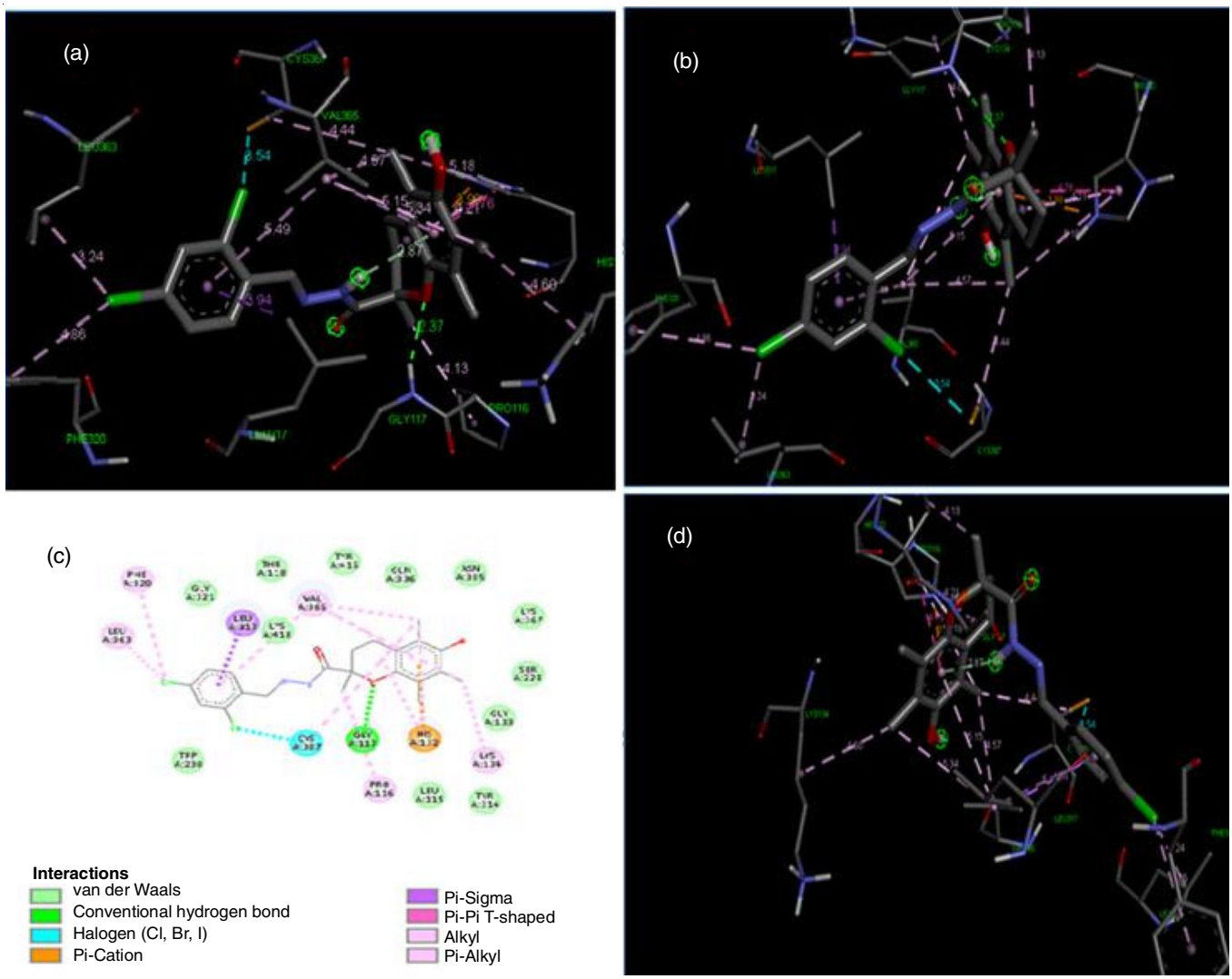

Fig. 2. Binding interactions of the docked ligand **SM8** with the target protein (PDB ID: 3PTY)

from the two chlorine atoms present at the non-chroman benzene ring with the residues GLY-921 and TRP-1057 with a bond distance of 2.94 and 4.25 Å, respectively.

Binding interaction of SM9 with target protein (PDB ID: 3PTY): As shown in Fig. 3a-c, compound **SM9** has shown the best binding interaction with the target protein (PDB ID: 3PTY). It was observed that it formed two hydrogen bond interactions with the TYR-17 residue of the target protein. One of the two hydrogen bonds increased from the nitrogen of the N-N-C=O moiety and another one was raised from the oxygen of the carbonyl group of N-N-C=O moiety. The bond length was calculated to be 2.65 and 2.58 Å, respectively. Three alkyl bonding interactions were also raised from methyl groups of the benzene ring of chroman and increased to the ALA-98, ALA-101 and LEU-188 amino acid residues of the target proteins.

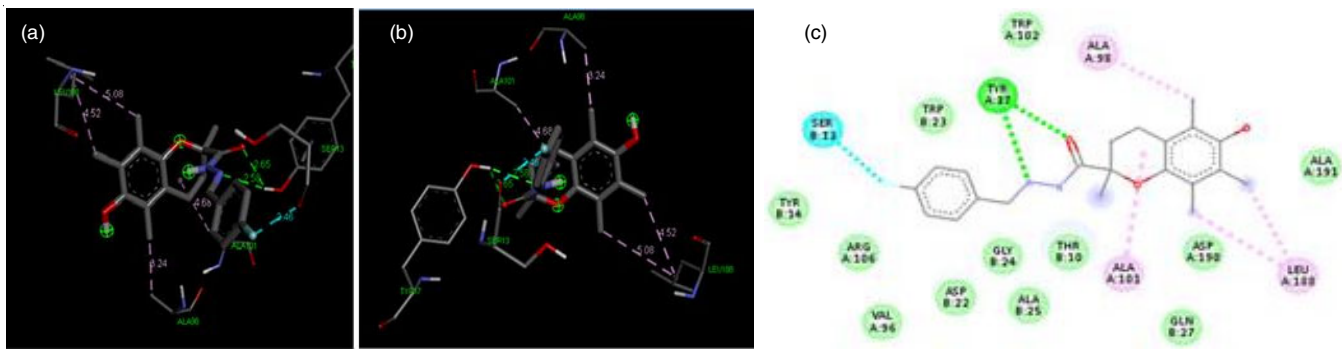

Fig. 3. Binding interactions of the docked ligand **SM9** with target protein (PDB ID: 3PTY)

Binding interaction of SM4 with target protein (PDB ID: 4FDO): As depicted in Fig. 4a-c, compound **SM4** has shown the best binding interaction with the target protein (PDB ID: 4FDO). It formed eight alkyl binding interactions with ALA-120, PRO-110, ILE-125, PHE -72, LEU-20, PHE-72, LYS-70 and HIS-126 residue of the target protein. These interactions were raised from the methyl groups and non-chroman benzene of the molecule. Pi-sigma bonding interaction was also raised from the benzene ring of the chroman moiety and increased to VAL-68 residue of the target protein with a bond distance of 3.84 Å.

***In silico* predicted ADME studies:** ADME properties of compounds (**SM1-SM10**) such as gastro-intestinal absorption, P-glycoprotein inhibiting property, blood-brain barrier crossing ability along with drug-likeness prediction such as Lipinski, Ghose and Veber rules and bioavailability score were predicted by online tool Swiss-ADME and results are presented in Table-3. All the compounds displayed high gastro-intestinal absorption except compound **SM5**. Compounds **SM6**, **SM9** and **SM11** showed blood-brain barrier permeability. None of the synthesized compounds was found to be the inhibitor of cytochrome P450 isomers CYP1A2 and CYP2D6 (inhibition of these isoenzymes is a prime cause of pharmacokinetics-related drug interactions). Except for compound **SM5**, all others followed Lipinski's rule of five, Ghose rule and Veber rule. All of the compounds have shown a good bioavailability score.

***In silico* predicted toxicity studies:** Toxicity prediction studies were performed by Osiris Property Explorer and results are presented in Table-4. Mutagenic (MUT) and tumorigenic (TUMO) ability was predicted by utilizing Osiris molecular property explorer. Green colour illustrates low toxicity, orange colour illustrates moderate toxicity and red colour illustrates high toxicity. Compounds with high Log P (CLP) values demonstrate low hydrophilicity and lead to poor drug absorption and permeation. Compounds **SM2**, **SM3**, **SM4**, **SM9** and **SM10** have shown better solubility parameters than any other compound, whereas compounds **SM1**, **SM2**, **SM6**, **SM7**, **SM8**, **SM9** and **SM10** showed positive DL values and compounds **SM3**, **SM4** and **SM15** have displayed significant CLP values. Compounds **SM1**, **SM4**, **SM5** and **SM6** have given the best drug score among all the compounds of the series.

Conclusion

In this work, new chroman-hydrazone derivatives were synthesized and characterized. All the compounds were in good agreement with all the spectral analyses. All compounds showed good binding scores with the target proteins, some of them (**SM4** and **SM9**) even gave better binding scores than standard drug isoniazid. Most of the compounds were found to be active inhibitors and gave good anti-tubercular activities such as **SM8** with MIC =16 µg/mL and **SM4** and **SM7** with MIC = 32 (µg/mL) each. It can be concluded that these compounds

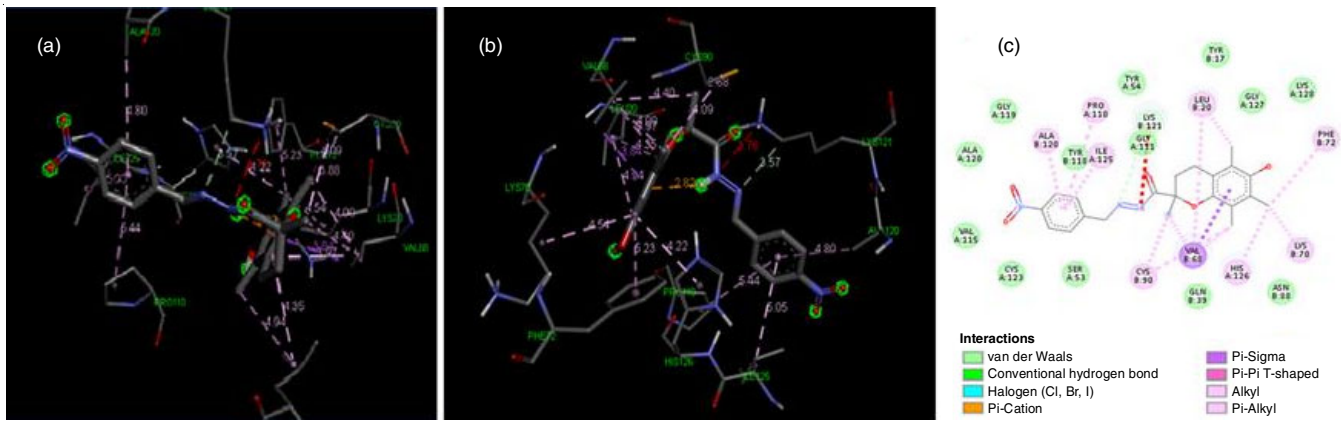

Fig. 4. Binding interactions of the docked ligand **SM4** with the target protein (PDB ID: 4FDO)

TABLE-3
RESULTS OF *in silico* PREDICTED ADME STUDIES

Code	Pharmacokinetics						Drug-likeness			
	GI absorption	BBB permeation	P-gp	CYP1A2	CYP2D6	Log Kp (cm/s)	Lipinski	Ghose	Veber	Bioavailability score
SM1	High	No	No	No	No	-4.98	Yes	Yes	Yes	0.55
SM2	High	No	No	No	No	-5.65	Yes	Yes	Yes	0.55
SM3	High	No	No	No	No	-5.85	Yes	Yes	Yes	0.55
SM4	High	No	No	No	No	-5.85	Yes	Yes	Yes	0.55
SM5	Low	No	Yes	No	No	-4.58	No	No	No	0.17
SM6	High	Yes	No	No	No	-5.44	Yes	yes	yes	0.55
SM7	High	Yes	No	No	No	-5.22	Yes	yes	yes	0.55
SM8	High	No	No	No	No	-4.98	Yes	Yes	Yes	0.55
SM9	High	Yes	No	No	No	-5.49	Yes	Yes	Yes	0.55
SM10	High	No	Yes	No	No	-6.00	Yes	Yes	Yes	0.55

GI: Gastro Intestinal; P-gp: P-glycoprotein; BBB: Blood Brain Barrier; CYP1A2: Cytochrome P450 family 1 sub-family. A member 2 (PDB: 2HI4); CYP2D6: Cytochrome P450 family 2 subfamily D member 6 (PDB: 5TFT).

TABLE-4
RESULTS OF *in silico* PREDICTED TOXICITY STUDIES

Compd.	Toxicity risks		Osiris calculations				
	MUT	TUMO	MW	CLP	S	DL	D-S
SM1	Green	Green	420.0	5.53	-6.52	4.29	0.17
SM2	Green	Green	382.0	4.25	-5.06	3.36	0.33
SM3	Green	Green	397.0	3.40	-5.50	-1.63	0.20
SM4	Green	Green	397.0	3.40	-5.50	-6.68	0.17
SM5	Green	Green	430.0	5.04	-5.88	-0.13	0.18
SM6	Green	Green	430.0	5.04	-5.88	0.22	0.19
SM7	Green	Green	386.0	4.92	-5.78	4.19	0.27
SM8	Green	Green	420.0	5.53	-6.52	4.37	0.21
SM9	Green	Green	370.0	4.42	-5.36	2.55	0.31
SM10	Green	Orange	398.0	3.90	-4.76	3.96	0.29

could be employed as lead for designing of newer anti-tubercular drugs.

ACKNOWLEDGEMENTS

The authors express their gratitude towards Integral University, Lucknow and Hygia Institute of Pharmaceutical Education and Research, Lucknow, India for providing the necessary research facilities. The authors are also thankful to the SAIF unit, Central Drug Research Institute, Lucknow, India for their assistance in spectral data analysis and anti-tubercular evaluation. The manuscript number provided by the Research and Development Committee, Integral University, Lucknow is IU/R&D/2022-MCN0001749.

CONFLICT OF INTEREST

The authors declare that there is no conflict of interests regarding the publication of this article.

REFERENCES

1. WHO, Global Tuberculosis Control a Short Update to the 2019 Report, World Health Organization, Geneva (2019); https://www.who.int/tb/publications/global_report/en/
2. C. Sacchettini, E.J. Rubin and J.S. Freundlich, *Nat. Rev. Microbiol.*, **6**, 41 (2008); https://doi.org/10.1038/nrmicro1816
3. M.V. De Souza, *Recent Patents Anti-Infect. Drug Disc.*, **1**, 33 (2006); https://doi.org/10.2174/157489106775244163
4. M.V. De Souza, *Curr. Opin. Pulm. Med.*, **12**, 167 (2006); https://doi.org/10.1097/01.mcp.0000219264.42686.c9
5. F. Annunziata, C. Pinna, S. Dallavalle, L. Tamborini and A. Pinto, *Int. J. Mol. Sci.*, **21**, 4618 (2020); https://doi.org/10.3390/ijms21134618
6. K. Upadhyay, A. Bavishi, S. Thakrar, A. Radadiya, H. Vala, S. Parekh, D. Bhavsar, M. Savant, M. Parmar, P. Adlakha and A. Shah, *Bioorg. Med. Chem. Lett.*, **21**, 2547 (2011); https://doi.org/10.1016/j.bmcl.2011.02.016
7. A.H. Rezayan, P. Azerang, S. Sardari and A. Sarvary, *Chem. Biol. Drug Des.*, **80**, 929 (2012); https://doi.org/10.1111/cbdd.12044
8. E. Pini, G. Poli, T. Tuccinardi, L.R. Chiarelli, M. Mori, L. Costantino, A. Gelain, S. Villa, F. Meneghetti and D. Barlocco, *Molecules*, **23**, 1506 (2018); https://doi.org/10.3390/molecules23071506
9. C. Loncle, J.M. Brunel, N. Vidal, M. Dherbomez and Y. Letourneux, *Eur. J. Med. Chem.*, **39**, 1067 (2004); https://doi.org/10.1016/j.ejmech.2004.07.005
10. S.K. Sridhar, S.N. Pandeya, J.P. Stables and A. Ramesh, *Eur. J. Pharm. Sci.*, **16**, 129 (2002); https://doi.org/10.1016/S0928-0987(02)00077-5
11. S.G. Küçükgüzel, A. Mazi, F. Sahin, S. Öztürk and J.P. Stables, *Eur. J. Med. Chem.*, **38**, 1005 (2003); https://doi.org/10.1016/j.ejmech.2003.08.004
12. A.R. Todeschini, A.L.P. de Miranda, K.C.M. da Silva, S.C. Parrini and E.J. Barreiro, *Eur. J. Med. Chem.*, **33**, 189 (1998); https://doi.org/10.1016/S0223-5234(98)80008-1
13. S. Eswaran, A.V. Adhikari, N.K. Pal and I.H. Chowdhury, *Bioorg. Med. Chem. Lett.*, **20**, 1040 (2010); https://doi.org/10.1016/j.bmcl.2009.12.045
14. K.K. Bedia, O. Elcin, U. Seda, K. Fatma, S. Nathaly, R. Sevim and A. Dimoglo, *Eur. J. Med. Chem.*, **41**, 1253 (2006); https://doi.org/10.1016/j.ejmech.2006.06.009
15. J. Vinsová, A. Imramovský, J. Jampílek, J.F. Monreal and M. Dolezal, *Anti-Infect. Agents Med. Chem.*, **7**, 12 (2008); https://doi.org/10.2174/187152108783329780
16. A. Nayyar, A. Malde, E. Coutinho and R. Jain, *Bioorg. Med. Chem.*, **14**, 7302 (2006); https://doi.org/10.1016/j.bmc.2006.06.049
17. A. Daina, O. Michielin and V. Zoete, *Sci. Rep.*, **7**, 42717 (2017); https://doi.org/10.1038/srep42717
18. J. Eberhardt, D. Santos-Martins, A.F. Tillack and S. Forli, *J. Chem. Inf. Model.*, **61**, 3891 (2021); https://doi.org/10.1021/acs.jcim.1c00203
19. O. Trott and A.J. Olson, *J. Comput. Chem.*, **31**, 455 (2010); https://doi.org/10.1002/jcc.21334
20. D.S. Biovia, Discovery Studio Modeling Environment, Dassault Syst. Release, San Diego, USA (2017).
21. S.M. Batt, T. Jabeen, V. Bhowruth, L. Quill, P.A. Lund, L. Eggeling, L.J. Alderwick, K. Fütterer and G.S. Besra, *Proc. Natl. Acad. Sci. USA*, **109**, 11354 (2012); https://doi.org/10.1073/pnas.1205735109
22. L.J. Alderwick, G.S. Lloyd, H. Ghadbane, J.W. May, L. Eggeling, A. Bhatt, K. Fütterer and G.S. Besra, *PLoS Pathog.*, **7**, e1001299 (2011); https://doi.org/10.1371/journal.ppat.1001299
23. J.A. Hyatt, *Synth. Commun.*, **38**, 8 (2007); https://doi.org/10.1080/00397910701648728
24. P. Rawat and S.M. Verma, *Drug Des. Devel. Ther.*, **10**, 2779 (2016); https://doi.org/10.2147/DDDT.S111266
25. M.C.S. Lourenço, M.V.N. Souza, A.C. Pinheiro, M.L. Ferreira, R.S.B. Gonçalves, T.C.M. Nogueira and M.A. Peralta, *ARKIVOC*, 181 (2007); https://doi.org/10.3998/ark.5550190.0008.f18